

# LIFETIME OF THE $^{99}\text{Rh}$ $7/2_1^+$ STATE FROM FAST-TIMING MEASUREMENTS\*

IR.B. VASILEV<sup>a</sup>, S. KISYOV<sup>b</sup>, S. LALKOVSKI<sup>a</sup>, N. MĂRGINEAN<sup>c</sup>  
C. MIHAI<sup>c</sup>, L. ATANASOVA<sup>d</sup>, D. BUCURESCU<sup>c</sup>, GH. CĂTA-DANIL<sup>c</sup>  
I. CĂTA-DANIL<sup>c</sup>, D. IVANOVA<sup>e,f</sup>, R. LICA<sup>c</sup>, N. FLOREA<sup>c</sup>  
R. MĂRGINEAN<sup>c</sup>, A. NEGRET<sup>c</sup>

<sup>a</sup>Faculty of Physics, Sofia University “St. Kl. Ohridski”, Sofia 1164, Bulgaria

<sup>b</sup>Lawrence Berkeley National Laboratory, Berkeley, CA 94720, USA

<sup>c</sup>Horia Hulubei National Institute for R&D in Physics and Nuclear Engineering  
Măgurele 077125, Romania

<sup>d</sup>Medical University — Sofia, Sofia 1431, Bulgaria

<sup>e</sup>Military Medical Academy, Sofia 1606, Bulgaria

<sup>f</sup>University Hospital “Prof. Alexander Tschirkov”, Sofia 1431, Bulgaria

*Received 10 November 2023, accepted 13 January 2024,  
published online 24 April 2024*

The structure of the lowest-lying positive-parity states in  $^{99}\text{Rh}$  was studied via in-beam fast-timing measurements performed with the hybrid ROSPHERE multidetector array. The half-life  $T_{1/2} = 405(20)$  ps, obtained for the  $7/2_1^+$  state, suggests that the M1 component of the  $7/2_1^+ \rightarrow 9/2_1^+$  transition is hindered with respect to the single-particle estimates by two orders of magnitude, while the E2 component is enhanced, similarly to other odd- $A$  nuclei in this region.

DOI:10.5506/APhysPolBSupp.17.3-A6

## 1. Introduction

Over the last decade, the structure of the lowest-lying excited states in  $A \sim 100$  nuclei was systematically studied [1–3] via a recently developed in-beam fast-timing method [4], sensitive to picosecond lifetimes of excited nuclear states. The method has opened new opportunities to study the evolution of collectivity. In-beam fast-timing measurements were previously performed to investigate a number of odd-mass Ru [2], Pd [1], and Cd [3] nuclei enabling a more detailed systematic study of the nuclear structure at low excitation energies. With the present study, we extend this research by presenting new data on  $^{99}\text{Rh}_{54}$ , and the  $7/2_1^+$  state in particular. This state

\* Presented at the XXXVII Mazurian Lakes Conference on Physics, Piaski, Poland, 3–9 September, 2023.

appears close to the lowest-lying positive-parity state  $9/2^+$ . Similar states are observed in the odd- $A$  Ag nuclei [5] which is somewhat surprising given that different mechanisms generate these states in Rh and Ag. In  $^{97}\text{Ag}$ , the yrast states arise from the  $\pi g_{9/2}^{-3}$  configuration, while in  $^{99}_{45}\text{Rh}_{54}$ , having more valence particles, respective states should arise from collectivity.

Indeed,  $^{99}\text{Rh}$  is placed in a mass region where the onset of quadrupole deformation emerges. This transition is now well-established in the even-even systems, where comprehensive nuclear data exist. There, the onset of the quadrupole deformation is indicated by the  $E_{2+}$  level energy systematics, reduced transition strengths, and last but not least, by the experimental quadrupole moments. In the odd- $A$  nuclei, the rise of collectivity is more elusive given the larger number of excited states at lower energies, which makes the problem more difficult to tackle, what makes the matter even worse is the general scarcity of experimental data. Often, to deduce the reduced transition strengths, not only lifetime data are needed but also multipolarity mixing ratios are necessary.

To get a deeper insight into the structural changes in the  $A \sim 100$  odd- $A$  nuclei, we have performed a fast-timing experiment on  $^{99}\text{Rh}$  aiming at measuring the half-life of the  $7/2^+$  state. This quantity can provide a deeper insight not only into the  $^{99}\text{Rh}$  structure itself, but also on the evolution of collectivity into the  $A \sim 100$  odd-mass nuclei.

## 2. Experiment

The  $^{99}\text{Rh}$  nuclei were produced in fusion–evaporation reaction with the  $^{102}\text{Rh}$  compound nucleus formation. The experiment was performed at the 9-MV IFIN-HH Tandem accelerator, where  $^6\text{Li}$  beam was accelerated to 32 MeV and impinged on a 10 mg/cm<sup>2</sup> thick  $^{96}\text{Mo}$  target. The  $^{99}\text{Rh}$  nuclei were produced via the  $^{96}\text{Mo}(^6\text{Li}, 3n\gamma)$  reaction channel, and the  $\gamma$  rays were detected by the hybrid ROSPHERE multidetector array comprising 11  $\text{LaBr}_3:\text{Ce}$  and 14 HPGe. The system was triggered by triple coincidences between two  $\text{LaBr}_3:\text{Ce}$  and one HPGe detectors, allowing for unambiguous selection of the reaction channel and  $\gamma$ -decay path [4]. In this experiment,  $2 \times 10^7$  triple coincidences were recorded.

In addition, fold-2 events were also recorded to monitor the experiment and for spectroscopic studies. A high-resolution  $\gamma$ – $\gamma$  matrix was constructed and investigated for coincidences. A partial decay scheme of  $^{99}\text{Rh}$ , as observed in the present experiment, is presented in Fig. 1 (a).

To select the reaction channel and the decay path of interest, HPGe gated  $E\gamma$ – $E\gamma$ – $T$  matrices were constructed by following the procedures described in Refs. [3, 4]. In the present study, the reaction channel producing  $^{99}\text{Rh}$  was selected by choosing only the events where the  $\gamma$  rays shown in Fig. 1 (a)

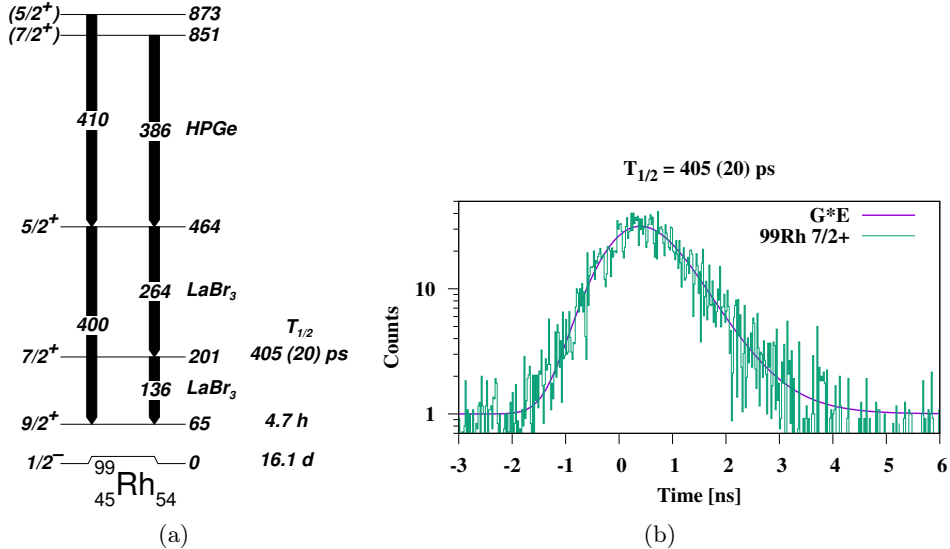


Fig. 1.  $^{99}\text{Rh}$  data from the present experiment. (a) Partial  $\gamma$ -decay scheme of  $^{99}\text{Rh}$ . (b) Experimental time spectrum of the  $^{99}\text{Rh}$   $7/2^+$  state ( $^{99}\text{Rh}$   $7/2^+$ ), gated on 386 keV  $\gamma$  ray detected by any of the HPGe detectors, and the 264 and 136 keV  $\gamma$  rays detected by the LaBr<sub>3</sub>:Ce detectors. The convoluted spectrum ( $G \star E$ ) is also shown.

were detected. The  $7/2^+$  state in  $^{99}\text{Rh}$  is fed by a 264 keV transition and decays to the 65 keV  $9/2^+$  isomeric state via a 136 keV transition. Also, the  $5/2^+$  state at 464 keV is populated via two transitions with energies of 410 and 386 keV. Thus, the  $7/2^+$  time spectrum, shown in Fig. 1(b), was constructed from an  $E_\gamma$ - $E_\gamma$ - $T$  matrix. The matrix is constructed under the condition of the 386 keV  $\gamma$  ray being detected by any of the ROSPHERE's HPGe detectors. Then, to produce the time spectrum, the  $E_\gamma$ - $E_\gamma$ - $T$  matrix was gated on the 264 and 136 keV  $\gamma$  rays and projected on the time axis. The half-life of  $T_{1/2} = 405(20)$  ps was obtained by fitting the experimental time spectrum with the convoluted function ( $G \star E$ )

$$G \star E = \int_{-\infty}^{+\infty} n(x' - x; \mu, \sigma^2) \exp(x; \lambda) dx,$$

where  $n(x' - x; \mu, \sigma^2)$  and  $\exp(x; \lambda)$  are the normal and exponential distributions, where the free parameters ( $\lambda, \mu, \sigma^2$ ) were determined from a least-squares fit to the experimental data. The convolution method was invoked

because of a relatively long tail observed in the time spectrum, suggesting that the lifetime of the state is of the order of the time resolution of the system [6].

### 3. Discussion

The neutron mid-shell Rh nuclei are long sought to be a textbook example of rigid triaxiality. The Particle plus Rigid Triaxial Rotor model calculations describe well the experimental data on odd- $A$  rhodium nuclei [7, 8]. Additionally, band structures are observed in some Rh nuclei that can be associated with spontaneous chiral symmetry breaking [9], which further supports the triaxial shape interpretation. On the neutron deficient side, when approaching the  $N = 50$  shell closure at  $^{97}\text{Rh}$ , collectivity decreases. Similar trends are observed in the Ag and In isotopic chains, as shown in Fig. 2. Thus, the  $^{99}_{45}\text{Rh}_{54}$  is placed on the limit between the two regimes defined by the shell model and the particle-plus-rotor model. To test the collectivity in  $^{99}\text{Rh}$  at low excitation energies, reduced electromagnetic transition strengths were calculated and compared to those in analogous transitions in neighbouring odd-mass Tc, Rh, and Ag nuclei given in Table 1.

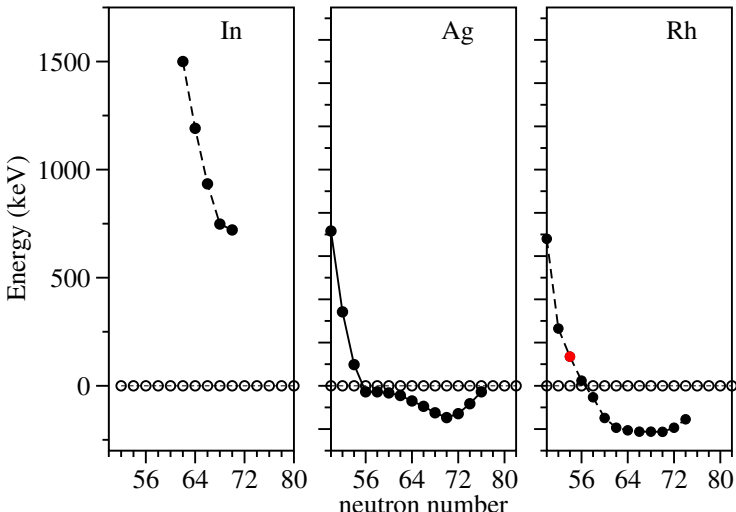


Fig. 2. (Colour on-line) Systematics of  $9/2^+$  (open circles) and  $7/2^+$  (full circles) in indium ( $^{49}\text{In}$ ), silver ( $^{47}\text{Ag}$ ), and rhodium ( $^{45}\text{Rh}$ ) isotopic chains. The red/grey dot denotes the  $7/2^+$  state of interest in  $^{99}\text{Rh}$ .

The  $^{99}\text{Rh}$  reduced transition probabilities  $B(\text{M1}; 7/2^+ \rightarrow 9/2^+) = 0.0179(17)$  W.u. and  $B(\text{E2}; 7/2^+ \rightarrow 9/2^+) < 132$  W.u., respectively, were deduced by using the mixing ratio  $\delta = 0.2(2)$  and the electron conversion coefficient  $\alpha$  which were taken from Ref. [10]. Due to the large uncertainty

on the mixing ratio  $\delta$ , we only give an upper limit of  $B(\text{E}2)$ , which makes it difficult to draw firm conclusions on the strength. However, the present data suggest that, most likely, the transition is of collective nature. What also emerges from the present study is that the magnetic dipole transition is hindered by two orders of magnitude with respect to the Weisskopf estimates, while the  $B(\text{E}2)$  value is likely enhanced. Similar strengths are also observed in other neighbouring neutron-deficient (Fig. 3) Ag, Rh, and Tc isotopes as shown in Table 1. Thus, the  $^{99}\text{Rh}$  low-lying positive parity states show signatures of collectivity similar to that in the  $^{97}\text{Tc}$ ,  $^{101}\text{Rh}$ , and  $^{105}\text{Ag}$  nuclei.

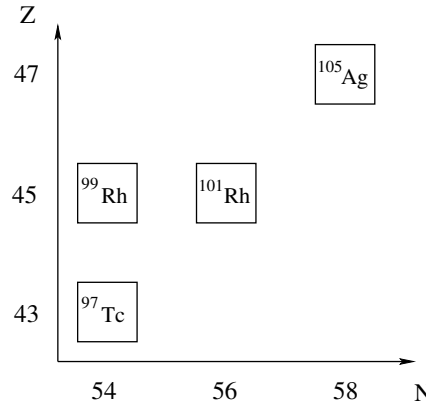


Fig. 3. Segment of the chart of nuclei with  $^{97}\text{Tc}$ ,  $^{99}\text{Rh}$ ,  $^{101}\text{Rh}$ , and  $^{105}\text{Ag}$  denoted.

Table 1. Properties of the low-energy positive-parity states and their decay modes in selected  $A \sim 100$  nuclei.

Nucleus	$E_i$	$J_i^\pi$	$E_\gamma$	$\delta$	$\alpha$	$B(\text{M}1)$	$B(\text{E}2)$
Ref.	[keV]	[\hbar]	[keV]			[W.u.]	[W.u.]
$^{97}_{43}\text{Tc}_{54}$	216	$7/2^+$	216	0.27 (2)	0.0378 (7)	0.029 (8)	43 (14)
[11]							
$^{99}_{45}\text{Rh}_{54}$	201	$7/2^+$	136	0.20 (20)	0.16 (3)	0.0179 (17)	< 132
[10]							
$^{101}_{45}\text{Rh}_{56}$	157	$7/2^+$	24	0.020 (6)	20.8 (1)	0.0361 (11)	22 (13)
[12]							
$^{105}_{47}\text{Ag}_{58}$	53	$9/2^+$	28	0.044 (8)	17.5 (3)	0.0241 (10)	53 (20)
[13]							

#### 4. Conclusion

The  $^{99}\text{Rh}$  level scheme shows some similarities with those of neutron-deficient Ag nuclei, where the ground state is  $9/2^+$  and the first excited state is  $7/2^+$ , suggesting that these nuclei have a similar structure at low energies. The lifetime measurements performed in the present study are consistent with the systematics, showing that the  $B(\text{M1})$  value is reduced by two orders of magnitude with respect to the single-particle estimates. A similar hindrance is observed for the M1 component of the same transition in  $^{97}\text{Tc}$  and  $^{101}\text{Rh}$ . The  $B(\text{E2})$  component of this transition cannot be precisely determined due to the large uncertainty on the mixing ratio but the transition most likely has an enhanced collective component, suggesting that the collectivity in odd- $A$  Rh nuclei arises already in  $^{99}\text{Rh}$ .

This work is partially supported by the Bulgarian National Science Fund under contract number KP-06-N68/8. S.L. effort is funded by the European Union — NextGenerationUE, the National Recovery and Resilience Plan of the Republic of Bulgaria, project No. BG-RRP-2.004-0008-C01.

#### REFERENCES

- [1] D. Ivanova *et al.*, *Phys. Rev. C* **105**, 034337 (2022).
- [2] S. Kisyov *et al.*, *Bulg. J. Phys* **42**, 583 (2015).
- [3] S. Kisyov *et al.*, *Phys. Rev. C* **84**, 014324 (2011).
- [4] N. Marginean *et al.*, *Eur. Phys. J. A* **46**, 329 (2010).
- [5] S. Lalkovski, S. Kisyov, *Phys. Rev. C* **106**, 064319 (2022).
- [6] T. Newton *et al.*, *Phys. Rev.* **79**, 490 (1950).
- [7] T. Venkova *et al.*, *Eur. Phys. J. A* **6**, 405 (1999).
- [8] S. Lalkovski *et al.*, *Phys. Rev. C* **88**, 024302 (2013).
- [9] J. Timár *et al.*, *Phys. Lett. B* **598**, 178 (2004).
- [10] E. Browne, J. Tuli, *Nucl. Data Sheets* **145**, 25 (2017).
- [11] N. Nica, *Nucl. Data Sheets* **111**, 525 (2010).
- [12] J. Blachot, Data extracted from the ENSDF database, 2006.
- [13] S. Lalkovski, J. Timár, Z. Elekes, *Nucl. Data Sheets* **161–162**, 1 (2019).